



ELSEVIER

Applied Surface Science 90 (1995) 419–423

applied
surface science

Range profiles of 6–10 MeV ^{15}N ions implanted in silicon

T. Ahlgren*, K. Väkeväinen, J. Räisänen, E. Rauhala, J. Keinonen

Accelerator Laboratory, P.O. Box 9, University of Helsinki, FIN-00014 Helsinki, Finland

Received 7 April 1995; accepted for publication 14 July 1995

Abstract

Implantation profiles of 6 to 10 MeV ^{15}N ions in crystalline silicon have been investigated. Measurements of the profiles at depths from 4 to 7 μm were rendered possible by combining the depth profiling of the ^{15}N atoms through the $^{15}\text{N}(\text{p}, \alpha\gamma)^{12}\text{C}$ reaction and the exfoliation of the surface layer of the samples, accomplished by high dose ^4He ion bombardment. In this way the range profiles, measured at the exfoliated crater bottom, could be obtained accurately without uncertainties due to straggling of the probing proton beam. The range parameters are compared to those of Monte Carlo calculations using the electronic stopping powers given by J.F. Ziegler, J.P. Biersack and U. Littmark [The Stopping Powers and Ranges of Ions in Matter, Vol. 1 (Pergamon, New York, 1985)]. Projected ranges were observed to be 5%–10% larger and range stragglings 27%–6% smaller than those predicted by Monte Carlo calculations along with the adopted stopping power parametrization.

1. Introduction

The ^{15}N ion range and the electronic stopping power of crystalline Si (c-Si) for 6–10 MeV ^{15}N ions is of significant importance due to their use in the depth profiling of hydrogen via the reaction $^1\text{H}(^{15}\text{N}, \alpha\gamma)^{12}\text{C}$. In materials processing by ion implantation, the knowledge of the slowing down and the range of the implanted ions is essential. Nitrogen in silicon has found a wide range of applications in semiconductor technology, e.g. deep nitrogen implants have been used for electrical isolation, nitride layers as impurity diffusion barriers, gate dielectrics, and interlevel passivators in integrated

circuit devices. In micromachining technology the use of hard nitride layers to increase mechanical strength is well known, e.g. for constructing corrosion, wear and oxidation resistant microscale structures. In many cases, ion implantation is an appropriate alternative in producing the nitride materials and doping of nitrogen into silicon.

Few studies of the slowing down of high energy nitrogen ions in c-Si have been presented in the literature [1–5]. In Refs. [1–3] some data on stopping powers in the energy range of 1–23 MeV were obtained. The projected ranges of ^{14}N ions in c-Si, measured by optical reflectivity measurements at bevelled samples have been reported in Ref. [1]. No previous nitrogen ion range distribution parameters have been published in the relevant energy region. In Refs. [4,5] the channeling effects and nitrogen concentration profiles of N^+ ions implanted in Si below 1.4 MeV were investigated.

* Corresponding author. Fax: +358 0 1918378; E-mail: tommy.ahlgren@helsinki.fi.

In the present study we introduce a new direct method for measuring the range distributions of high energy implantation of ^{15}N ions in c-Si. The nuclear resonance broadening (NRB) method and the $E_p = 429$ keV resonance in the reaction $^{15}\text{N}(p, \alpha\gamma)^{12}\text{C}$ is used for measuring the implanted ^{15}N concentration profiles. Due to the long range of the MeV ions, the direct use of the NRB method is not feasible. The significant energy straggling of the probing protons at depths extending up to $10\ \mu\text{m}$ and the interference from a second resonance at $E_p = 900$ keV, would render accurate depth profiling by the NRB method impractical. Therefore, the exfoliation phenomenon was taken advantage of for making the silicon layer thinner above the implanted nitrogen concentration profile. In this way the effect of straggling and the uncertainty in the stopping power of the probing beam is minimized in deducing the range parameters. Due to blistering, measurable craters are produced in the silicon samples bombarded with hydrogen or helium ions [6]. The crater depths corresponding to the projected range are then measured by a profilometer.

The experimental range parameters are compared with those obtained in transport equation (the PRAL code) [7] and Monte Carlo calculations (the TRIM code) [7]. Both theoretical range calculations rely on the stopping power given in the parametrization (ZBL-85) by Ziegler, Biersack and Littmark [8].

2. Experimental

The ^{15}N ion implantations at 6–10 MeV were carried out by using the 5 MV tandem accelerator EGP-10-II at the laboratory. The ^1H and ^4He ion beams were obtained from the 2.5 MV Van de Graaff accelerator of the laboratory.

The silicon samples were n-type Si(100) slices (Czochralski grown, doped uniformly by P to a resistivity of $2.5\text{--}3.5\ \Omega\cdot\text{cm}$). Doses of 1×10^{16} ^{15}N ions cm^{-2} were implanted into the samples at room temperature and at an angle of 7° with respect to the normal of the sample surface. To study the dependence of the resulting implantation distributions on sample orientation versus beam alignment, some of the samples were tilted at 7.0° and rotated continuously around an axis perpendicular to the sample

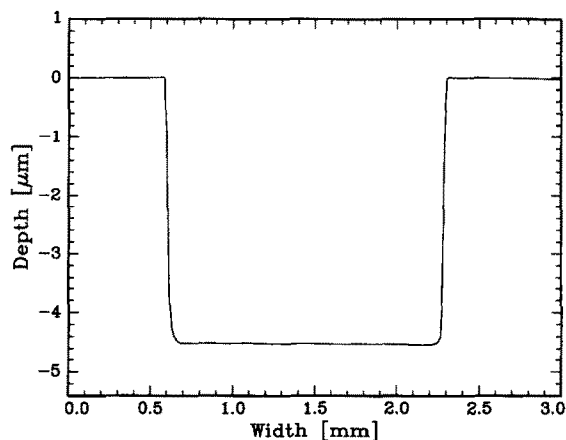


Fig. 1. A crater profile measured with the profilometer for the 6 MeV implanted sample.

surface during implantations. With this procedure an orientation as close to random as possible was obtained.

The craters of required depth were obtained by bombarding the Si samples by $1.25\text{--}1.90$ MeV ^4He ions at room temperature at an angle of 7° with respect to the normal of the sample surface. Ion currents of 1.5 to $0.5\ \mu\text{A}$ and doses of 4.5 to 8 mC were used. No change in the underlying ^{15}N range profile was observed when the ^4He ion implantation parameters were varied. The exfoliation procedure has been investigated in more detail in Refs. [6] and [9]. The crater depths were measured by an absolutely calibrated Dektak IIA surface profilometer [9]. A crater profile for the 6 MeV implanted sample is shown in Fig. 1. The depth uniformity of the crater bottom (average roughness) was typically less than 0.5%. In some cases, small shoulders above the surface level at the rim of the craters were observed. These effects amounted to less than 3% of the crater depth.

The concentration profiles of ^{15}N were measured by NRB using the $E_p = 429$ keV resonance in the reaction $^{15}\text{N}(p, \alpha\gamma)^{12}\text{C}$. The beam resolution was about 500 eV and the natural width of the resonance was $\Gamma = 124$ eV [10], corresponding to the depth resolving power of about 3 nm at the sample surface. The gamma-rays in a suitable energy window were detected with a 12.7 cm (diameter) \times 10.2 cm NaI(Tl) detector.

3. Results

The experimental ^{15}N ion implantation profiles and Pearson-IV distributions fitted to the profiles are plotted in Fig. 2. The depth scale of the concentration distributions was obtained using the stopping powers of Si for protons from Ref. [8]. The projected ranges R_p and the higher moments, range straggling (standard deviation) σ and skewness γ , derived from the deconvoluted distributions are presented in Tables 1 and 2.

The uncertainties in the range values obtained arise from the possible errors in determining the crater depths, the uncertainty of the proton stopping power and the Pearson-IV distribution fitting procedure. The uncertainty of the average depth of the craters as obtained by the profilometer and the depth scale of the NRB ranges fall below 3% and 5%, respectively. This results in estimated errors of the positions of the range profiles below 3%.

To extract the concentration distribution of ^{15}N from the experimental data, the data were deconvoluted by an instrument function composed of the straggling and beam resolution contributions. We have observed that Bohr energy straggling [11] has to be multiplied by a factor of 0.9 for 600 keV protons in silicon [12]. This is in accordance with the models of Lindhard and Scharff [13] and Chu [14]. We have adopted this correction to Bohr straggling in the deconvolution of the range profiles.

The extension of the distribution to higher depths

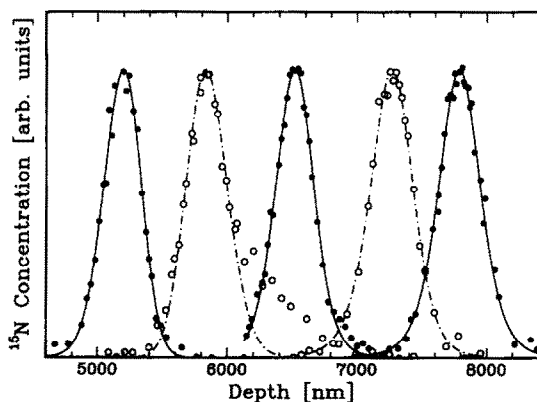


Fig. 2. The experimental ^{15}N ion implantation profiles and the Pearson-IV distributions fitted to the data. From left to right, the implanted ^{15}N ion energies are 6, 7, 8, 9, and 10 MeV.

Table 1

Projected ranges R_p of ^{15}N ions in silicon

Energy (MeV)	Crater depth (μm)	Mean depth of the range profile (μm)	Projected range, R_p (μm)
6	4.56 ± 0.14	0.617 ± 0.03	5.18 ± 0.14
7	5.00 ± 0.15	0.842 ± 0.05	5.84 ± 0.16
8	6.12 ± 0.18	0.390 ± 0.02	6.51 ± 0.18
9	6.44 ± 0.19	0.813 ± 0.04	7.25 ± 0.20
10	6.70 ± 0.20	1.080 ± 0.06	7.78 ± 0.21

The crater depth corresponds to the depth of the exfoliated region of the sample, measured by a profilometer. The mean depth of the range profile is derived from the Pearson-IV distributions, fitted to the experimental profiles, measured at the exfoliated region; R_p is the sum of the two contributions.

Table 2

Higher moments, range straggling (standard deviation) σ and skewness γ as derived from the deconvoluted Pearson-IV distributions and a comparison to parameters from Monte Carlo calculations (TRIM)

Energy (MeV)	Range straggling (nm)		Skewness	
	Expt.	TRIM	Expt.	TRIM
6	138	176	-0.36	-8.0
7	151	172	0.17	-6.5
8	162	179	-0.16	-5.5
9	175	186	-0.29	-5.0
10	186	199	-0.27	-6.0

beyond the modal range, the high energy tail, is evident in some of the profiles of Fig. 2. This effect is due to the channelled fraction of the beam. Despite

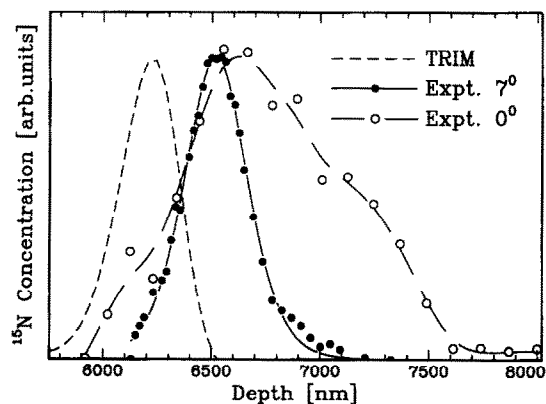


Fig. 3. The experimental 8 MeV ^{15}N profiles implanted at 7° (with sample rotation), and 0° (without rotation) with respect to the normal of the sample surface, along with the Monte Carlo (TRIM) distribution calculations.

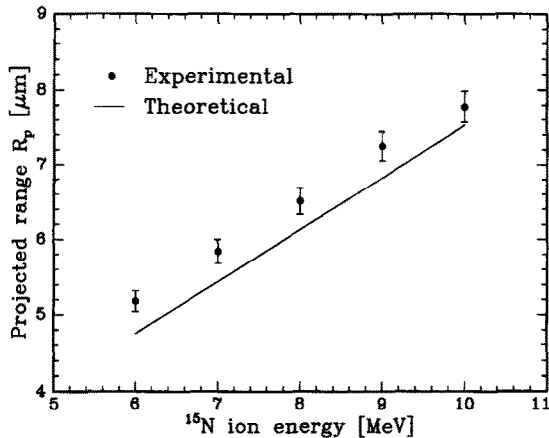


Fig. 4. Projected ranges of ^{15}N ions in silicon and comparisons to theoretical calculations (TRIM and PRAL).

tilting and rotation, a small fraction of the beam still follows planar and axial channelling trajectories in a single crystal target. We did not observe a significant difference in the tails between the implantations performed with and without sample rotation. In order to study the effect of the channeled fraction to the depth profile, some implantations were performed without rotation and at an angle of incidence of 0° . For these implantations, prominent tails due to channelling were observed in the implanted ion distributions. Fig. 3 compares the 8 MeV ^{15}N profiles implanted at 7° (with sample rotation) and 0° (without rotation) along with the profile obtained in the Monte Carlo calculations.

The observed range values for the projected range together with those obtained on the Monte Carlo (the TRIM code) and transport equation (the PRAL code) calculations are shown in Fig. 4.

4. Discussion

The difference between the two theoretical projected range calculations is found to be negligible. We observe that the present projected range data exceed the calculated values by 10%–5%, the difference decreasing with increasing ion energy. This indicates that below 6 MeV, ZBL-85 overestimates the average stopping by 10%. Between 6 and 10 MeV, the average energy loss in the energy intervals

7 to 6 MeV, 8 to 7 MeV, 9 to 8 MeV, and 10 to 9 MeV are found to be 1.52, 1.49, 1.35, and 1.89 MeV/ μm , respectively. The corresponding ZBL-85 values for 6.5, 7.5, 8.5, and 9.5 MeV are 1.45, 1.44, 1.43, and 1.42 MeV/ μm , respectively. The average experimental stopping power between 6 and 10 MeV is 5% higher than that predicted by ZBL-85, i.e. ZBL-85 underestimates the stopping power in this energy region.

Bussmann et al. [1] report projected ranges for 1–23 MeV ^{14}N ions in silicon. When the mass difference between ^{15}N and ^{14}N is taken into account the reported values of 5.00, 6.43, and 7.88 μm for 6, 8, and 10 MeV for ^{14}N ions, respectively, are in good agreement with the present results.

Bussmann et al. [1] also calculate stopping powers from their ^{14}N ion range data. At energies below 7.5 MeV their stopping powers fall below the ZBL-85 predictions. From 7.5 MeV to 23 MeV their data increasingly exceed the predictions up to about 10% at 23 MeV. Demond et al. [2] report a value of 1.44 ± 0.07 MeV/ μm for 6.4 MeV ^{15}N ions in a good agreement with the ZBL-85 value of 1.45 MeV/ μm . Bulgakov et al. [3] have reported an energy loss of 1.45 ± 0.12 MeV/ μm for 4.75 MeV nitrogen ions incident on 2.5 μm Si. We calculated that this is about 4% less than the ZBL-85 value of 1.51 MeV/ μm for the mean energy of 2.9 MeV. The stopping power values reported in the literature are consistent with our range measurements.

In the exfoliation method used, the straggling contribution of the probing proton beam has only a small effect to the observed range distribution. When deducing the moments for the 6 to 10 MeV ^{15}N implantation distributions, the proton straggling was corrected for the dissimilar mean depths of the range profiles (column three, Table 1). This effect is illustrated in Fig. 5, where the Pearson-IV distributions are compared for the two extreme cases, for depths of 0.39 and 1.1 μm . Bohr stragglings at 0.39 and 1.1 μm are 6.2 and 11 keV (full width at half maximum of the average energy loss fluctuation), respectively.

Due to the high implantation energies of 6 to 10 MeV, the nuclear straggling component in the total straggling contribution is similar in all our measurements. Consequently, the difference in the range straggling data is due to the difference in the electronic straggling component. For example from 10

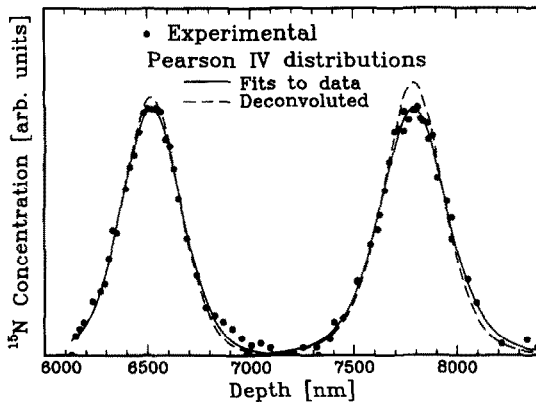


Fig. 5. The deconvoluted distributions for the 8 and 10 MeV implantations. The dots denote the experimental profiles. The solid lines are the Pearson-IV distributions fitted to the experimental profiles, the dashed lines the distributions without straggling and beam resolution contributions.

and 6 MeV energies, we get 48 nm as the electronic straggling for the relevant 4 MeV energy difference.

For the 6 to 10 MeV energies, we find 27%–6% smaller range straggling and significantly smaller skewness than obtained by the Monte Carlo calculations. In comparison to the calculations, the difference in the straggling data is larger than the 10%–5% difference in the stopping powers. No straggling data for nitrogen ions in the present energy region can be found in the literature.

To conclude, a new method to measure implantation profiles of MeV energy implants in semiconductors is introduced to obtain accurate range profiles. It

is utilized to determine the range distribution parameters of 6–10 MeV ^{15}N ions in c-Si.

References

- [1] U. Bussman, N. Hecking, K.F. Heidemann and E. Te Kaat, Nucl. Instr. Meth. B 15 (1986) 105.
- [2] F.-J. Demond, S. Kalbitzer, J. Mannsperger and G. Müller, Nucl. Instr. Meth. 168 (1980) 69.
- [3] Yu. Bulgakov, V.S. Nikolaev and V.I. Shulga, Phys. Lett. A 46 (1974) 477.
- [4] A. Gasparotto, A. Garnera, S. Acco and A. La Ferla, Nucl. Instr. Meth. B 62 (1992) 356.
- [5] A. Gasparotto, A. Garnera, S. Acco and A. La Ferla, in: Crucial Issues in Semiconductor Materials and Processing Technologies, Proc. NATO Adv. Study Inst. on Semiconductor Materials and Processing Technologies (Kluwer, Dordrecht, 1992) pp. 213–217.
- [6] E. Rauhala and J. Räsänen, Nucl. Instr. Meth. B 94 (1994) 245.
- [7] J.F. Ziegler and J.P. Biersack, TRIM-92 (version 92.04), private communication (1992). See also: J.P. Biersack, Nucl. Instr. Meth. 182/183 (1981) 199; Z. Phys. A 305 (1982) 95.
- [8] J.F. Ziegler, J.P. Biersack and U. Littmark, The Stopping and Range of Ions in All Elements (Pergamon, New York, 1985).
- [9] J. Räsänen and E. Rauhala, Nucl. Instr. Meth. B 93 (1994) 1.
- [10] T. Osipowicz, K.P. Lieb and S. Brussermann, Nucl. Instr. Meth. B 18 (1987) 232.
- [11] N. Bohr, K. Dan. Vidensk. Selsk. Mat. Fys. Medd. 18 (1948) 8.
- [12] J. Keinonen, A. Kuronen, K. Nordlund, R.M. Nieminen and A.P. Seitsonen, Nucl. Instr. Meth. B 88 (1994) 382.
- [13] J. Lindhard and M. Scharff, K. Dan. Vidensk. Selsk. Mat. Fys. Medd. 27 (1953) 15.
- [14] W.K. Chu, Phys. Rev. A 13 (1976) 2057.